J. Korean Earth Sci. Soc., v. 43, no. 4, p. 511−519, August 2022
https://doi.org/10.5467/JKESS.2022.43.4.511

ISSN 1225-6692 (printed edition)
ISSN 2287-4518 (electronic edition)

Two Overarching Teleconnection Mechanisms Affecting the Prediction of the 2018 Korean Heat Waves

Jieun Wie and Byung-Kwon Moon*

Division of Science Education & Institute of Fusion Science, Jeonbuk National University,
Jeonju 54896, Korea

Abstract: Given the significant social and economic impact caused by heat waves, there is a pressing need to predict them with high accuracy and reliability. In this study, we analyzed the real-time forecast data from six models constituting the Subseasonal-to-Seasonal (S2S) prediction project, to elucidate the key mechanisms contributing to the prediction of the recent record-breaking Korean heat wave event in 2018. Weekly anomalies were first obtained by subtracting the 2017-2020 mean values for both S2S model simulations and observations. By comparing four Korean heat-wave-related indices from S2S models to the observed data, we aimed to identify key climate processes affecting prediction accuracy. The results showed that superior performance at predicting the 2018 Korean heat wave was achieved when the model showed better prediction performance for the anomalous anticyclonic activity in the upper troposphere of Eastern Europe and the cyclonic circulation over the Western North Pacific (WNP) region compared to the observed data. Furthermore, the development of upper-tropospheric anticyclones in Eastern Europe was closely related to global warming and the occurrence of La Niña events. The anomalous cyclonic flow in the WNP region coincided with enhancements in Madden-Julian oscillation phases 4-6. Our results indicate that, for the accurate prediction of heat waves, such as the 2018 Korean heat wave, it is imperative for the S2S models to realistically reproduce the variabilities over the Eastern Europe and WNP regions.

Keywords: Korean heat waves, Eastern European anticyclonic anomaly, western North Pacific upward motion, Subseasonal-to-Seasonal Prediction (S2S) Model

Introduction

Heat waves cause abnormally high temperatures, with adverse effects on human health, as well as difficulties in daily livelihoods of people and socio-economic damage (Son et al., 2012; Kim et al., 2016; Campbell, 2018; Xu et al., 2016). The Korea Meteorological Administration issues heat wave advisories and warnings to reduce damage when high temperatures are expected to persist over a long period. The damage caused by heat waves is characterized by the significance of severe damage to socially vulnerable groups, such as the low-income class and rural areas, who cannot take proper responsive measures against the situation of heat waves. According to a study on heatwaves, the intensity of Korean heatwaves has shown a gradually increasing trend, and the number of days of heatwave events has also increased. Among the numerous heat wave events that struck the Korean Peninsula, the 2018 Korean heat wave recorded the highest temperature, longest duration, and longest duration of tropical nights, resulting in 44,094 cases of heat-related illnesses and 145 heat-related deaths. (Chae et al., 2020). Additionally, given the global warming phenomenon, the frequency of heat wave events will increase, and the intensity of heat waves is also expected to increase due to the increasing humidity and the increasing air temperature (Stocker et al., 2013; Shin et al., 2018; Min et al., 2020; Ha et al., 2022).

To reduce the damage from heat waves and establish adequate preparations, previous studies have investigated regional factors influencing Korean heat waves (Wie

---

*Corresponding author: moonbk@jbnu.ac.kr
Tel: +82-63-270-2824

et al., 2021; Yoon et al., 2018). For example, the foehn winds by the mountains on the east coast of the Korean Peninsula considerably increase the surface air temperature (SAT), thus influencing the generation of heat waves in the western region of the Korean Peninsula. Additionally, the ocean surrounding the Korean Peninsula plays an important role (Wie et al., 2021). Moreover, urban developments crowded with man-made buildings experience higher temperatures because of the heat island effect (Kim et al., 2021b; Yi et al., 2022). Recent studies have investigated teleconnection patterns that cause heatwaves in the Korean Peninsula. For example, Yeh et al. (2018) presented a mechanism for the development of Korean heat waves based on increased anticyclonic activity (high geopotential height) on the Kamchatka Peninsula and strong convective activity in the western North Pacific (WNP). Yeo et al. (2019) proposed the zonal wave (Z-wave), a wave propagation pattern from Europe through Central Asia to East Asia, and a meridional wave (M-wave) propagating from the WNP to East Asia as patterns of Korean heat waves. Kim et al. (2021a) additionally proposed cluster 3 (C3)-type heat waves, a pattern of wave trains propagating from Eastern Europe, in addition to C1 and C2, similar to the Z-wave and M-wave. Kim et al. (2019) proposed a heat wave mechanism by diabatic heating propagating from northern Pakistan to northwestern India (PWI) in northern India, the Tibetan Plateau, and East Asia. These heat wave mechanisms can be summarized and classified as follows: Rossby wave propagation from the Silk Road region, atmospheric waves propagating from Eastern Europe, development of anticyclonic anomalies on the Korean Peninsula due to enhanced convection in the WNP, and the development of East Asian anticyclones caused by diabatic heating from the PWI region.

From the previous studies, it is clear that a reliable prediction of Korean heat waves can be achieved if subseasonal-to-seasonal (S2S) prediction models can reproduce the abovementioned heat wave processes. Based on this expectation, this study aimed to identify the heat wave mechanism that is closely related to the heat wave prediction performance of S2S prediction models for the 2018 extreme heat wave event on the Korean Peninsula.

The remainder of this study is organized as follows. The model and observation data used in this study are outlined in Section 2. In Section 3, the prediction performance of the models used for SAT over the Korean Peninsula for the period of July and August 2018 is analyzed. Section 4 presents an analysis of two different heat wave mechanisms closely associated with the performance of the Korean heat wave prediction by the S2S models. Section 5 presents a summary and conclusions of this study.

Data and Methods

The real-time data over the summer season (July-August) for the period 2017-2020 were analyzed for six models: China Meteorological Administration (CMA), Environment and Climate Change Canada (ECCC), European Center for Medium-Range Weather Forecasts (ECMWF), Korea Meteorological Administration (KMA), National Centers for Environmental Prediction (NCEP), and the United Kingdom's Met Office (UKMO) participating in the S2S prediction project. These S2S models were selected as they cover the common period (2017-2020). Depending on the model, prediction data were provided once a week, twice weekly, or daily. Thus, 7-day averages were calculated, and the analysis was performed from week 1 to week 4 prediction lead times.

For the observational data, the daily average NCEP2 reanalysis data were used. Similar to the model data described above, the surface temperature and geopotential height of July-August from 2017 to 2020 were converted into weekly data. The anomalies in 2018 were calculated by removing the average values for the period 2017-2020, considering only years when all real-time S2S forecasts are available. To analyze the heat wave mechanism, surface air temperature (SAT), geopotential height, and wind data from the NCEP2 reanalysis data and sea surface temperature (SST) data from optimum interpolation sea surface temperature

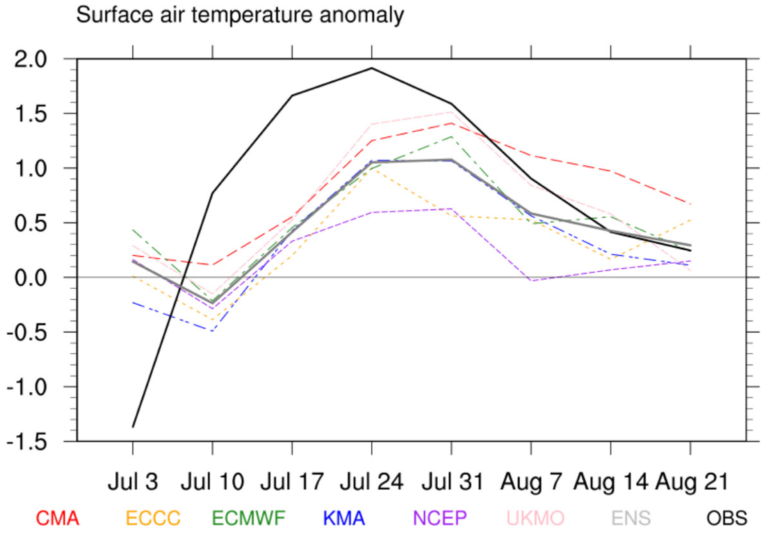

Fig. 1. Simulated weekly surface air temperature anomalies over the Korean Peninsula (124°E-131°E, 33°N-42°N) averaged for the lead time (1-4 weeks or 1-28 days) along with the observation (NCEP Reanalysis 2) data. Note that x-axis represents the starting day of each week.

(OISST) data were used. For the Madden-Julian Oscillation (MJO) index, real-time multivariate MJO was provided by the Bureau of Meteorology (downloaded from https://iridl.ldeo.columbia.edu/SOURCES/.BoM/.MJO/.RMM/).

For the Korean heat-wave mechanism indices, the geopotential anomalies associated with the development of Korean heat waves proposed in previous studies were used (Table 1). For example, for the generation of C3-type heat waves defined in Kim et al. (2021a), there was a dominant development of anticyclonic anomalies in eastern Europe (Fig. 2c in Kim et al., 2021a). Previously, we defined the heat wave index of C3 as an upper-level anticyclonic anomaly in eastern Europe. Similarly, in the case of diabatic heating over the Indian subcontinent (DHIS) index, the high-pressure anomalies in the northeastern PWI region were used to define the heat-wave index. For the M-wave and Z-wave, geopotential height values defined by Yeo et al. (2019) were also used. While the latter two indices include the geopotential height over the Korean Peninsula, the index in this study was calculated by excluding the region. To analyze the prediction performance of the 2018 Korean heat waves, pattern correlation, mean bias error (MBE), root mean square error (RMSE), and correlation coefficients were calculated. Additionally, a regression analysis was performed to identify the main mechanisms related to the prediction of Korean heat waves.

S2S model prediction performance for 2018 Korean heat waves

The Korean Peninsula (averaged over 124°E-131°E, 33°N-42°N) showed a long-term positive SAT anomaly from July 10 to the end of August 2018 (OBS in Fig. 1). The highest temperature anomaly was about 1.9°C, occurring on July 24-30. The S2S models simulated underestimated weekly SATs (cold biases) compared with the observation data, and the maximum anomaly value was the largest in UKMO, followed by CMA, ECMWF, ECCC, and NCEP. The simulated peaks of SAT anomalies were delayed compared to the observation data (Fig. 1).

Figure 2 shows the mean bias errors, root mean square errors, and correlation coefficients of surface air temperature over the Korean Peninsula. Note that Fig. 2 shows the lead time (1-4 weeks) averaged values as in Fig. 1. Most models have negative MBEs, except for the result obtained from CMA, reaffirming that most of the models predict undere-

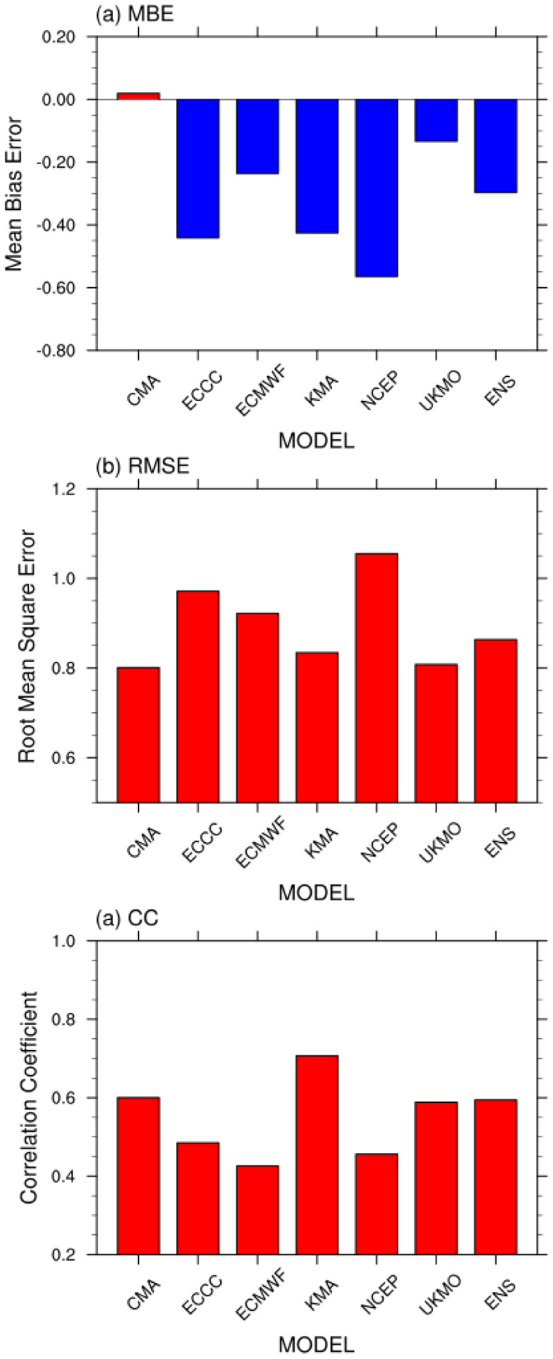

Fig. 2. Mean bias error, root mean square error, and correlation coefficient of surface air temperature over Korean Peninsula (124°E-131°E, 33°N-42°N) in S2S models from the average of lead time 1-4 weeks.

stimated SATs (Fig. 1). Notably, the CMA also exhibits the lower SAT than observation before July 31 but larger after that time in Fig. 1, leading to slight positive MBE of CMA (Fig. 2). Among the models, the CMA, UKMO, and ECMWF showed relatively small errors, whereas the ECCC, KMA, and NCEP exhibited large errors. With RMSE, the values obtained from CMA, KMA, and UKMO had the smallest errors, and the results from ECCC and NCEP had large errors. Based on the correlation coefficient analysis of the SAT time series for the period of July-August 2018 on the Korean Peninsula, the KMA, CMA, and UKMO models showed a high positive correlation, and the ECMWF and NCEP models showed a low correlation. Overall, it can be summarized that the predicted error is the smallest for KMA and UKMO models and the largest for ECCC and NCEP models.

As previous studies have demonstrated remote impacts (Kim et al., 2021a), Korean heat waves could be stronger because of the teleconnection influence from Europe. Figure 3 shows the distribution of SAT anomalies from a lead time of 4 weeks. Observation data indicate that high-temperature anomalies appear not only over the Korean Peninsula but also over the PWI region (Fig. 3f). Similarly, positive SAT anomalies were observed in northern and eastern Europe, indicating that there was also a significant temperature increase in these regions during the 2018 Korean heatwaves. The UKMO and ECMWF models captured these teleconnection patterns with the highest spatial correlation coefficients, whereas the CMA and ECCC showed low correlations.

Processes affecting predicting 2018 Korean heat waves

Figure 4 presents scatter plots of the four heat wave process indices versus SAT of the Korean Peninsula for July-August at a prediction lead time of 4 weeks. The four heat-wave indices are defined in Table 1. Our analysis does not determine the heat wave mechanism driving the 2018 Korean heat wave but identifies which processes are key to predicting the heat wave for S2S models. The observation data (four black dots in the figures) are all located in the upper

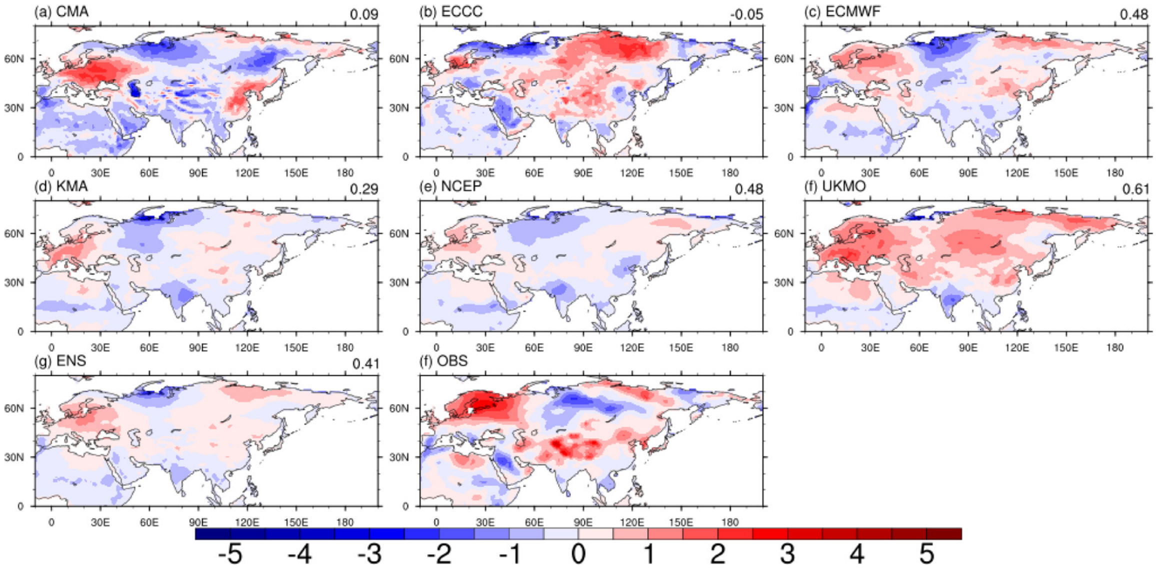

Fig. 3. Distribution of surface air temperature anomalies in week 4 in S2S models, with their spatial correlation coefficients against observation over the region of 10°W-200°E and 0-80°N.

right corner of each graph, indicating that the four processes are likely to contribute to the heat waves in the Korean Peninsula. Notably, the DHIS and Z-wave indices showed insignificant correlations. This indicates that the S2S models did not reproduce the observed DHIS and Z-wave contributions to the 2018 Korean heat wave.

However, as the S2S models are predicted so that the C3 index is close to the observation value, the SAT value will also become close to the observation data (Fig. 4a with a significantly correlation coefficient. The M-wave also had a significant positive correlation coefficient. The smaller error in C3 and M-wave indices seems to be the main reason for reliable temperature prediction in the Korean Peninsula. This also indicates that if the model is improved such that it is similar to the observed C3 and M-wave indices, the predicted SAT may be closer to the actual value.

To analyze the characteristics of the C3 and M-wave processes, which are important for the prediction of the 2018 heat waves in Korea, the SAT, C3 index, and M-wave index of July-August over the past 30 years are shown in Fig. 5. It can be seen that the SAT anomaly had a high value in 1994, and high-temperature events have frequently occurred after the 2010s. The Korean Peninsula experienced three strong heatwave events in 1994, 2016, and 2018. Considering the recent increase in high-temperature events, the figure shows that heat wave events have occurred frequently due to global warming. The C3 index shows a clear increasing trend and has the highest value in 2010, 2016, and 2018. The M-wave index had a positive value during the three major heat wave events in the Korean Peninsula.

Figure 6 shows the regression patterns of 200 hPa geopotential heights and sea surface temperatures on the C3 and detrended C3 indices. The C3 index showed an increasing trend; therefore, it was also analyzed using detrended values. Both indices showed wave propagation patterns in the mid-latitude regions, and anticyclonic activity was observed not only in Eastern Europe and the North Pacific region but also in the eastern United States and the North Atlantic regions, showing clear circumglobal teleconnection (CGT) patterns. The difference between the two indices appears in the atmospheric pressure above the North Pole, which is strongly correlated with the increasing C3 trend. In the case of SST, the C3 index

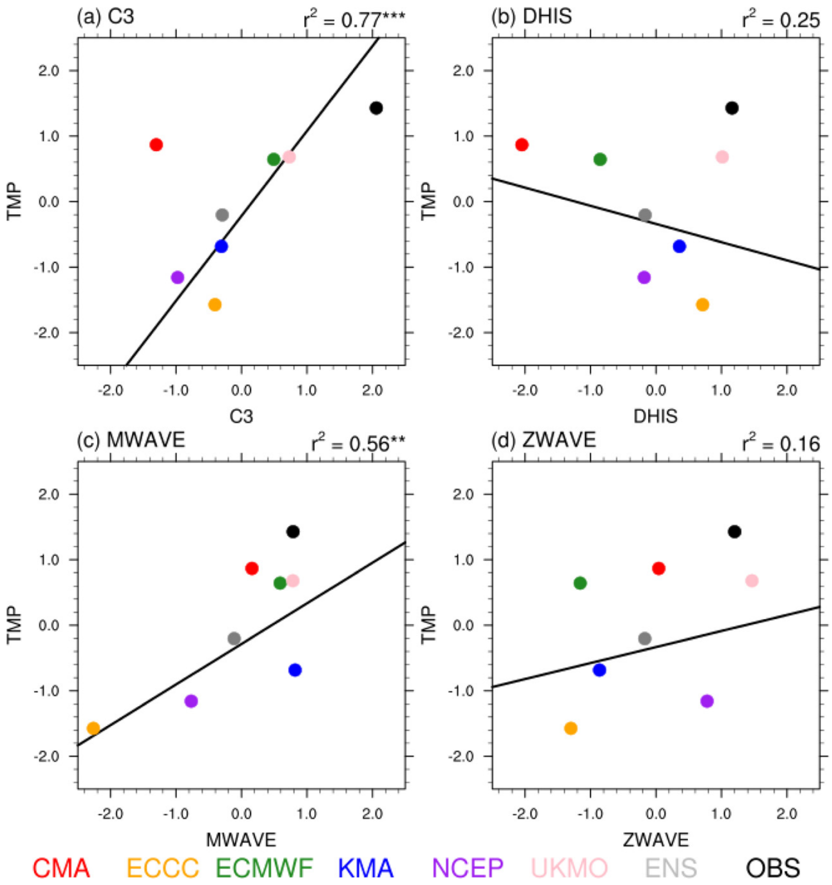

Fig. 4. Scatter plot of surface air temperature anomalies over the Korean Peninsula and heatwave mechanism indices of (a) C3, (b) DHIS, (c) M-wave, and (d) Z-wave. Black line indicates regressed line. The asterisks ** and *** indicate statistical significance at the 95% and 99% confidence level, respectively. The observation is excluded in the calculation of significance and coefficients of determination (r^2). The CMA's C3 index and temperature anomaly are also excluded in (a).

Table 1. Definitions of heatwave mechanism indices

Index	Definition	Variables	Reference
C3	Area_average (50°N-65°N, 45°E-75°E)	200 hPa GPH	Kim et al. (2021a)
DHIS	Area_average (30°N-45°N, 60°E-80°E)	200 hPa GPH	Kim et al. (2019)
M-wave	−1×Area_average (15°N-25°N, 120°E-150°E)	850 hPa GPH	Yeo et al. (2019)
Z-wave	Area_average (50°N-60°N, 10°E-40°E) -Area_average (45°N-55°N, 50°E-80°E)	850 hPa GPH	

is associated with SST warming in the western coastal regions of both hemispheres of the ocean. With the detrended index, the SST shows a negative anomaly along the equatorial Pacific region, indicating that the index is closely related to La Niña patterns.

The M-wave index is related to enhanced convection in the WNP, which lead to the development of anticyclones over the Korean Peninsula. The El Niño-Southern Oscillation (ENSO) and MJO variability are factors that modulate convection activities in this region. Wie et al. (2021) reported an enhancement in the tropospheric column ozone level owing to the development of anticyclones in East Asia in late spring to early summer after the La Niña phase in

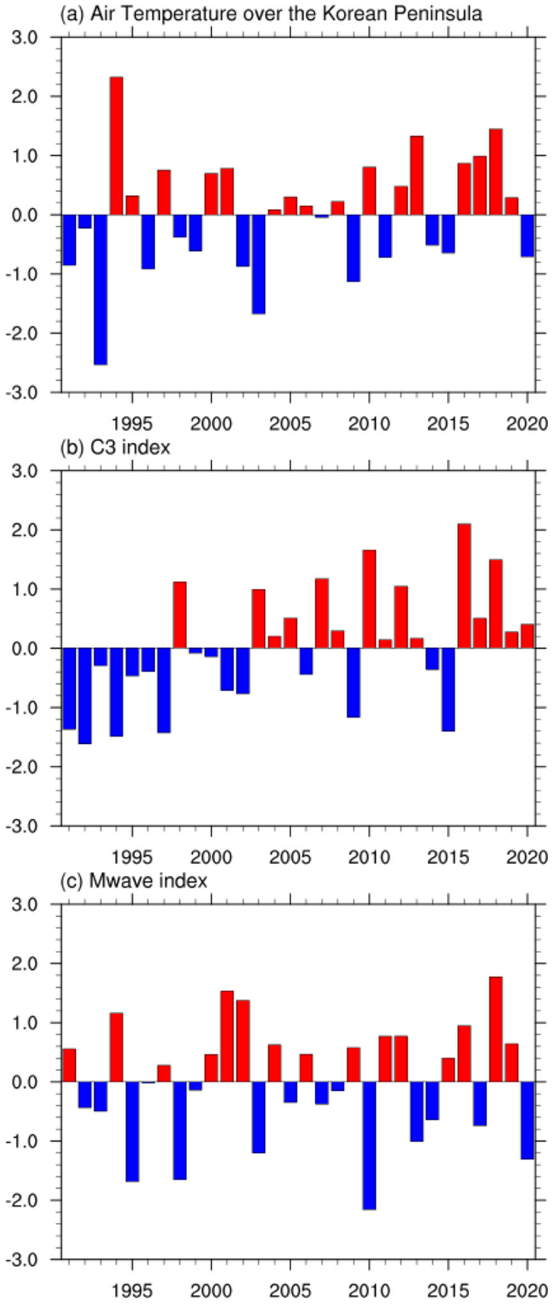

Fig. 5. Timeseries of 2-m temperature anomalies, and C3 and M-wave indices averaged in July and August for 1991-2020.

winter. Their simple numerical experiments also showed that when there is diabatic heating in the WNP, upward motion is induced, and in turn, downward motions are enhanced in the Korean Peninsula. Another factor is MJO activity (Hsu et al., 2020). In July-August 2018, more days were in MJO Phase 4-6 compared to the average value of July-August in 1991-2020 (Fig. 7a). According to the composite wind map and 850 hPa geopotential height in the days of MJO Phase 4-6 in July-August from 1991-2020, anomalous cyclonic circulations developed in the WNP and anticyclones were located in East Asia, indicating an environment where heat waves may be generated (Fig. 7b).

Conclusion

This study identified the heat wave processes most related to the prediction of the 2018 Korean heat waves by the S2S models and analyzed their long-term characteristics. The S2S models underestimated SAT during the summer season on the Korean Peninsula. The prediction performance of the S2S models for the 2018 Korean heat waves was closely related to the realistic reproduction of the increase in upper-tropospheric anticyclonic circulations in Eastern Europe. The Korean heat waves associated with the C3-type might be because of global warming with frequent occurrences in recent years (Kim et al. 2021a), and C3-related processes are expected to play a critical role in heat waves in the future warmer world. As the rate and patterns of global warming vary with time (Kosaka and Xie, 2013; Wie et al., 2014; Yan et al., 2016; Medhaug et al., 2017), it is necessary to develop strategies to apply these characteristics to S2S prediction models. For the M-wave process, it is important that the models properly reproduce the atmospheric variability in the tropical Pacific and Indian oceans, such as the ENSO and MJO, and the S2S variation of atmospheric circulations in East Asia. Our findings are expected to contribute to improving the prediction performance of Korean heat waves and enable adequate preparatory measures to prevent devastating damage from heat waves.

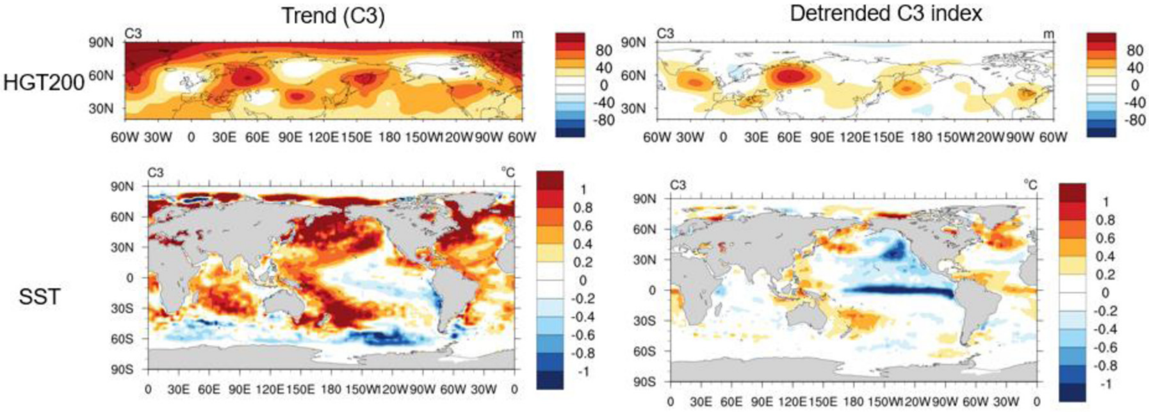

Fig. 6. Regression fields of 200 hPa geopotential height (upper) and SST (lower) onto trend (left) and detrended (right) C3 index in July and August for 1991-2020.

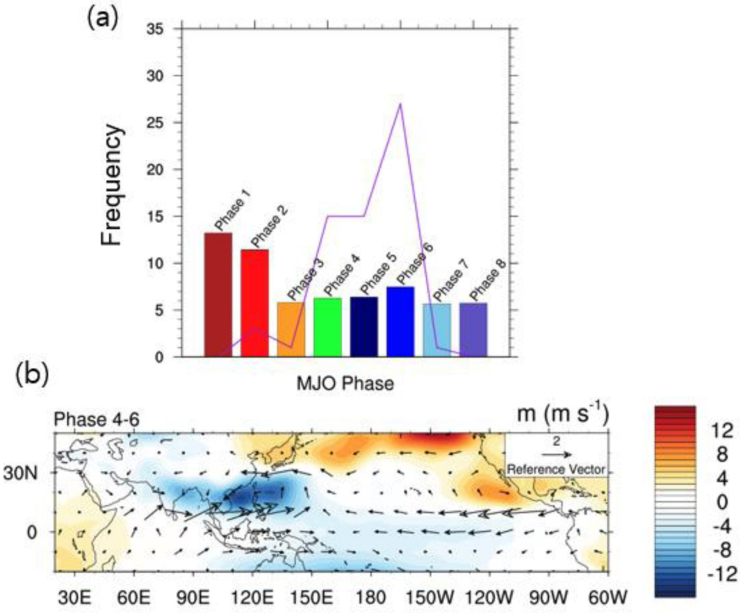

Fig. 7. (a) Frequency of each MJO phase in July and August in averaged period of 1991-2020 (bar plot) and 2018 (purple line). (b) Composite map of 850 hPa geopotential height (shaded, m) and wind (vector; m s^{-1}) in MJO phase 4-6 in July and August for 1991-2020.

Acknowledgments

This work was supported by the Korea Meteorological Administration Research and Development Program under Grant KMI2020-01212 and the National Research Foundation of Korea (NRF) grant funded by the Government of Korea (MSIT) (No. 2022R1A2C 1008858).

References

Campbell, S., Remenyi, T.A., White, C.J., and Johnston, F.H., 2018, Heatwave and health impact research: A global review. Health & Place 53, 210-218.

Chae, Y. et al., 2020, 2020 Heat Impact Report. Korea Environment Institute, Sejong, Korea, 34 p. (in Korean)

Ha, K.-J., Seo, Y.-W., Yeo, J.-H., Timmermann, A., Chung, E.-S., Franzke, C.L.E., Chan, J.C. L., Yeh, S.-W., and

Ting, M.F., 2022, Dynamics and characteristics of dry and moist heatwaves over East Asia. NPJ Climate and Atmospheric Science, 5, 49, doi:10.1038/s41612-022-00272-4.

Hsu, P.-C., Qian, Y., Liu, Y., Murakami, H., and Gao, Y., 2020, Role of abnormally enhanced MJO over the western Pacific in the formation and subseasonal predictability of record-breaking northeast Asian heatwave in the summer of 2018. Journal of Climate, 33, 3333-3349.

Kim, M.-K., Oh, J.-S., Park, C.-K., Min, S.-K., Boo, K.-O., and Kim, J.-H., 2019, Possible impact of the diabatic heating over the Indian subcontinent on heat waves in South Korea. International Journal of Climatology, 39, 1166-1180.

Kim, D.-W., Deo, R.C., Chung, J.-H., and Lee, J.-S., 2016, Projection of heat wave mortality related to climate change in Korea. Nature Hazards, 80, 623-637.

Kim, H.-K., Moon, B.-K., Kim, M.-K., Park, J.-Y., and Hyun, Y.-K., 2021a, Three distinct atmospheric circulation patterns associated temperature extremes in South Korea. Scientific Reports, 11, 12911, doi:10.1038/s41598-021-92368-9.

Kim, S.-W., Park, J., Kim, T., and Chae, Y., 2021b, Identification of heatwave hotspots in Seoul using high-resolution population mobility data. Urban Climate, 36, 100771, doi:10.1016/j.uclim.2021.100771

Kosaka, Y., and Xie, S.-P., 2013, Recent global-warming hiatus tied to equatorial Pacific surface cooling. Nature, 501, 403-407.

Medhaug, I., Stolpe, M.B., Fischer, E.M. Fischer, and Knutti, R., 2017, Reconciling controversies about the 'global warming hiatus'. Nature, 545, 41-47.

Min, S.-K., Kim, Y.-H., Lee, S.-M., Sparrow, S., Li, S., Lott, F.C., and Stott, P.A., 2020, Quantifying human impact on the 2018 summer longest heat wave in South Korea. Bulletin of the American Meteorological Society, 101, S103-S108, doi:10.1175/Bams-D-19-0151.1.

Shin, J., Olson, R., An, S.-I., 2018, Projected heat wave characteristics over the Korean Peninsula during the twenty-first century. Asia-Pacific Journal of Atmospheric Sciences, 54, 53-61.

Son, J.-Y., Lee, J.-T., Anderson, G. B., and Bell, M.L., 2012, The impact of heat waves on mortality in seven major cities in Korea. Environmental Health Perspectives, 120, 566-571.

Stocker, T.F. et al., 2013, Climate change 2013: the physical science basis. In Intergovernmental Panel on Climate Change, Working Group I Contribution to the IPCC Fifth Assessment Report (AR5). New York, NY: Cambridge University Press.

Wie, J., Moon, B.-K., Kim, K.-Y., and Lee, J., 2014, The global warming hiatus simulated in HadGEM2-AO based on RCP8.5. Journal of the Korean earth science society, 35, 249-258. (in Korean)

Wie, J., Moon, B.-K., Hyun, Y.-K., and Lee, J., 2021, Impact of local atmospheric circulation and sea surface temperature of the East Sea (Sea of Japan) on heat waves over the Korean Peninsula. Theoretical and Applied Climatology, 144, 431-446.

Xu, Z.W., FitzGerald, G., Guo, Y. M., Jalaludin, B., and Tong, S.L., 2016, Impact of heatwave on mortality under different heatwave definitions: A systematic review and meta-analysis. Environment International, 89-90, 193-203.

Yan, X.-H., Boyer, T., Trenberth, K., Karl, T.R., Xie, S.-P., Nieves, V., Tung, K.-K., and Roemmich, D., 2016, The global warming hiatus: Slowdown or redistribution? Earth's Future, 4, 472-482.

Yeh, S.-W., Won, Y.-J., Hong, J.-S., Lee, K.-J., Kwon, M., Seo, K.-H., and Ham, Y.-G., 2018, The record-breaking heat wave in 2016 over South Korea and its physical mechanism. Monthly Weather Review, 146, 1463-1474.

Yeo, S.-R., Yeh, S.-W., and Lee, W.-S., 2019, Two types of heat wave in Korea associated with atmospheric circulation pattern. Journal of Geophysical Research: Atmosphere, 124, 7498-7511.

Yi., C., Kwon, H.-G., Yang, H., 2022, Spatial temperature differences in local climate zones of Seoul metropolitan area during a heatwave. Urban climate, 41, 101012.

Yoon, D., Cha, D.-H., Lee, G., Park, C., Lee, M.-I., and Min, K.-H., 2018, Impacts of synoptic and local factors on heat wave events over southeastern region of Korea in 2015. Journal of Geophysical Research Atmospheres 123, 12081-12096.

Manuscript received: August 1, 2022
Revised manuscript received: August 27, 2022
Manuscript accepted: August 28, 2022